Massachusetts Institute of Technology
Cambridge, Massachusetts 02139

X-ray Imaging for Plasma Position Control in the Ignitor Experiment

F. Bombarda[1,3], E. Paulicelli[2], G. Pizzicaroli[1]

[1]*ENEA Frascati, Italy*
[2]*Università di Bari, Italy*
[3]*Massachusetts Institute of Technology, Cambridge, MA*

MIT (LNS) Report HEP 07/13

Cambridge, MA, December 2007

Physics of High Energy Plasmas

Thermonuclear Plasmas

Plasma Astrophysics

I. Introduction

The ignition experiment Ignitor [i] will produce, in high performance discharges, a neutron flux at the first wall comparable to that expected in future power producing reactors (~10^{15} n/cm^2/s). As a consequence, traditional magnetic diagnostics are expected to fail due to a sensible, although reversible, degradation of the inorganic insulators surrounding the conductors that are positioned in the shade of the Mo first wall tiles. The measurements of some fundamental plasma parameters, such as current and position, by means of electromagnetic diagnostics can thus become problematic. The control of the vertical plasma position is crucial in Ignitor as for every elongated plasma configuration, therefore the capability of the Poloidal Field Coils system to provide an effective vertical stabilization of the plasma column has been investigated, taking into account the possible failure of part of the electromagnetic diagnostic system, and it was found to be generally adequate [ii]. Nevertheless, an independent and complementary diagnostics should be available to provide the necessary signal redundancy, in case of a more extensive black-out of magnetic measurements. Since light extraction and detection will also be more difficult than in present day tokamaks, an alternative plasma position control method is proposed here, based on the diffraction and detection of soft X-ray radiation emitted near the top or bottom of the plasma column., where the distance of the Last Closed Magnetic Surface (LCMS) from the wall is only few millimeters.

The radiation emitted by the core plasma is, in general, a combination of continuous bremsstrahlung and line radiation, but the soft X-ray radiation from the edge is, in the case of Ignitor, mostly line radiation from Molybdenum. The Ignitor geometry allows the lower or upper sections of the plasma to be viewed from the horizontal ports. For the purpose of plasma position control, the system needs to be sufficiently fast (>1 kHz) and possibly provide an output signal to the control system without additional inputs from other diagnostics. The proposed layout is essentially an adaptation of the space resolving, curved crystal spectrometer in use on the FTU machine for ion temperature profile diagnostics from Doppler broadening measurements of highly ionized impurity lines. For the present application, however, high spectral resolution is not an essential requirement, whereas the spatial resolution needs to be relatively fine, of the order of few mm.

In the following sections the instrument design guiding lines are described, and then the detailed calculation for the geometrical parameters and estimated throughput are reported. The characteristics of the GEM detector are outlined, with the programmed development activities.

II. Plasma Model

The plasma LCMS in Ignitor is almost everywhere close to the first wall, which acts as an extended limiter (Fig. 1). This configuration has the advantage of spreading the thermal heat loads over a relatively large area, thus reducing the peak values. On the other hand, small errors in the position of the plasma column, of the order of 5 mm, or its sudden displacement, can produce "hot spots", or lead to the loss of vertical control, hence the need for an accurate localization of the plasma column.

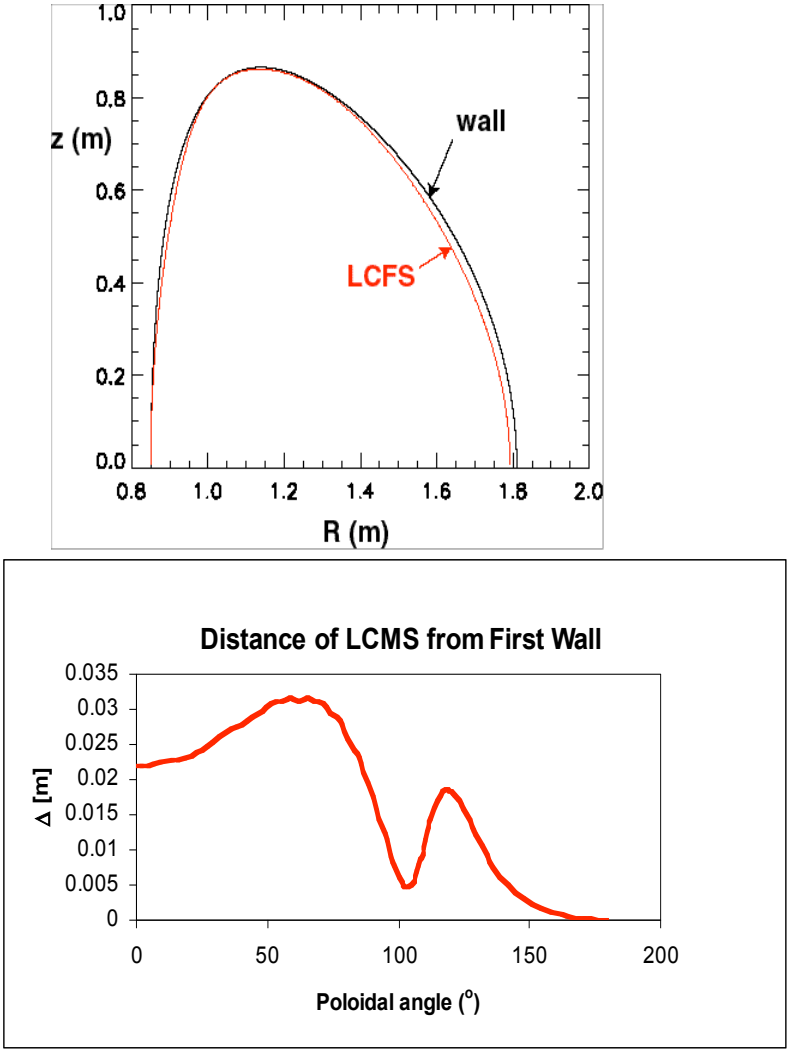

Figure 1 Plasma poloidal cross section in Ignitor (red) and distance of the Last Closed Magnetic Surface from the First Wall.

The tiles covering the plasma chamber will be made of TZM, a syntherized form of Mo. Thus, the radiation emitted from the edge plasma can be expected to be dominated by this

element, even if only a very small fraction of Mo ions (of the order of 10^{-5} times the electron density) enter the plasma. Other impurities are typically present in tokamak plasmas, namely carbon and oxygen, as well as lighter materials that may be used to condition the first wall, such as Be or Li. In fact, these medium or low Z elements are considerably more abundant than the metals (of the order of the percent), but since they get fully ionized at the very edge of the plasma, they radiate mostly by continuum bremsstrahlung. Their contribution to the radiated power is going to be included in this work through the global parameter $Z_{eff} \equiv \sum(n_Z Z^2)/\sum(n_z Z) = \sum(n_Z Z^2)/n_e$, which is a measure of the plasma purity. Extensive simulations have been carried out to determine both the core plasma parameters in the reference ignition scenario [i] and the edge plasma conditions [iii, iv] in Ignitor. The results that will be used in this work are summarized in Table I.

By taking into account magnetic equilibrium, temperature and density profiles at ignition, the total emissivity profiles for Mo, O, and C can be estimated. For light *Z* elements the cooling rate is estimated by using the Post-Jensen coefficients [v], but for Mo we have used the more recent and extensive calculation found in Ref. [vi]. We reproduce here Fig. 1 from [vi] to draw attention to the fact that the radiative losses from Mo are always dominated by collisional-radiative line emission, particularly at low temperatures, and that the emission reaches a maximum at around 50 eV and then drops sharply at higher temperature. We can exploit this steep sensitivity in correspondence to the region near or at the LCMS. Fig. 3 shows such profiles together with the contribution to the radiated power density, for reasonable assumptions regarding impurity concentrations and their distribution.

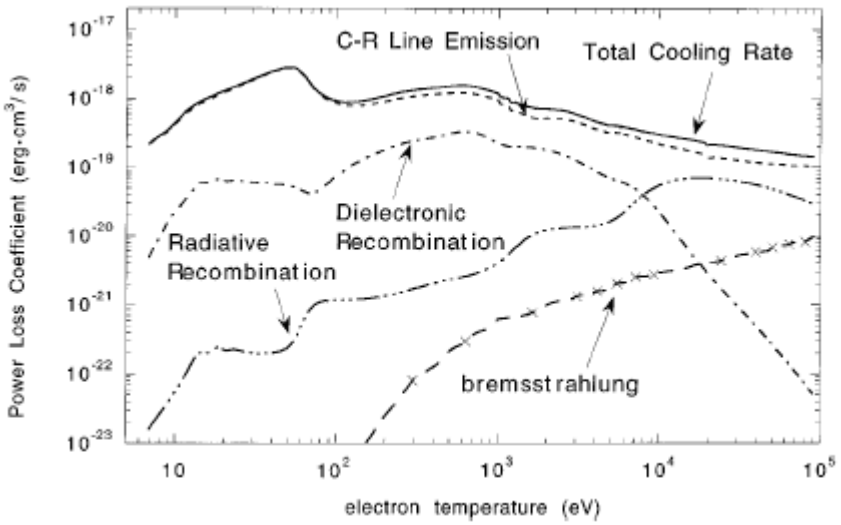

Figure 2 (From Fig. 1 of Ref vi) Comparison of radiative losses through collisionally excited line radiation (short dashes), dielectronic recombination line emission (dash-dot), radiative recombination continuum emission (dash-dot-dot-dot) and bremsstrahlung (broken line). Collisional-radiative line emission dominates the total cooling coefficient.

III. Instrument Lay-out

Conventional spectrometers in the Johann mounting make use of crystals bent to a radius of curvature $2R$, which define a focal circle (the Rowland circle) of radius R. Radiation of wavelength λ from an extended polychromatic source, located anywhere relative to the Rowland circle and the crystal, can be diffracted by the crystal if $\lambda = 2d \sin \vartheta_B$, where ϑ_B is the Bragg angle, and will be focused on the Rowland circle. Different wavelengths are focused at different locations; therefore an extended position sensitive detector placed on the Rowland circle can acquire a relatively broad spectral range simultaneously. The advantage of this mounting is that the whole crystal surface can contribute to the diffraction of any given wavelength, with very small aberrations if R is large. Luminosity therefore scales as $1/R$ instead of $1/R^2$ as typical of flat crystal spectrometers. The cylindrical Johann mounting is self-focusing in the (meridian) diffraction plane. In order to obtain a space resolved image of the plasma in the poloidal direction, a horizontal slit needs to be located between the crystal and the detector. A two-dimensional detector, such as a Multiwire Proportional Chamber, can thus record the spectra

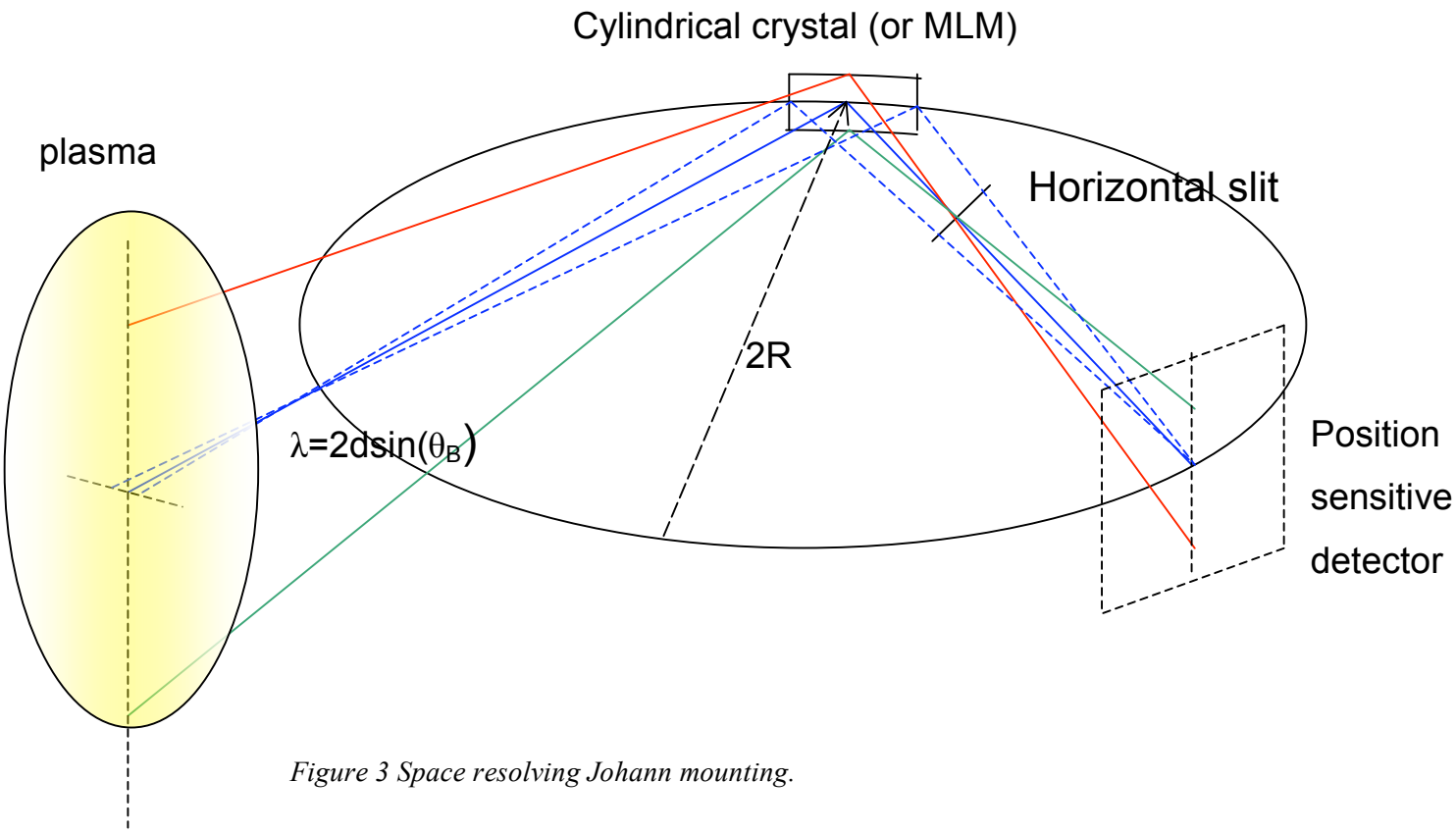

Figure 3 Space resolving Johann mounting.

along one dimension and the source distribution along the other (Fig. 3). This solution was adopted and successfully operated on the FTU machine [vii].

This new application requires the observation of the soft X-ray emission from the plasma edge, rather than from the plasma core as in the traditional ion temperature diagnostic set-up. The Ignitor horizontal port geometry, long and narrow, requires the diffracting element to be placed at a suitable location inside the port, and to be tilted towards the bottom (or the top) of the plasma column. Furthermore, for the radiation to be able to exit the port, the resulting Bragg angle has to be relatively shallow, requiring the use of Multilayer Mirrors (MLM) instead of natural crystals. The detailed calculations are reported in Appendix 1. The use of spherical mirrors [viii] is prevented, in the case of Ignitor, by the specific port geometry; toric mirrors, which would avoid the need for the slit, could be considered in successive optimization of the system design.

For radiation wavelengths of 20-50 Å thin Beryllium windows can still be used to separate the machine high vacuum from the rough vacuum in the detection arm that is attached to the external part of the port. The radiation can be detected by, for example, the new space resolving Gas Electron Multiplier (GEM) detectors [ix] outside the vessel, kept in indirect view of the plasma, where the front-end electronics can be properly protected. The high counting rates allowed by GEMs allow the possibility to detect any plasma movement with sufficient time resolution to be used for real-time feedback control of the vertical plasma position.

Two possible types of measurement are considered: the first adopts two symmetrical spectrometers, looking at the upper and lower regions of the plasma, respectively. The shift in vertical position is then deduced as a difference between the two signal intensities at each time. The second method relies on the time evolution of the signal from a single system pointed either to the top or the bottom. This will require a more sophisticated algorithm to distinguish signal changes associated with position shifts from variations of the background plasma parameters, but it offers the advantage of a simpler construction.

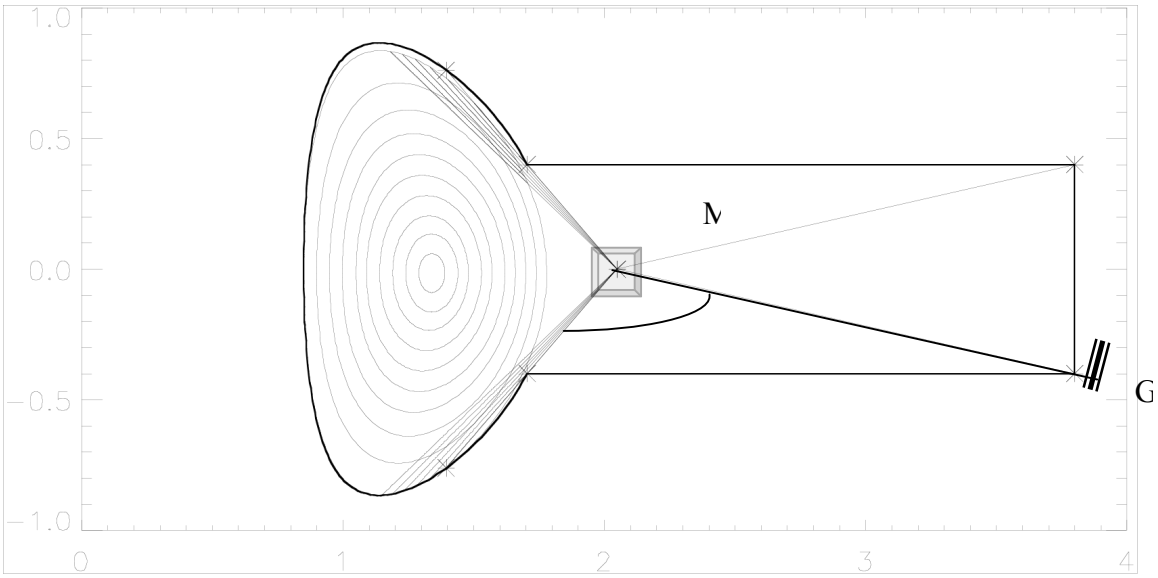

Figure 4 Two possible layouts are considered in this study: the first uses two identical spectrometer, one pointing to the upper part of the vacuum vessel, the other to the bottom. The control system compares the two signals at each time. The second method relies on the time history of the signal from a single instrument. It would require a more sophisticated algorithm but a simpler hardware.

IV. Plasma Radiation

The X-ray emission for Ignitor plasmas at ignition, both in the nominal extended limiter configuration and for a shifted plasma limited at the bottom of the first wall, but otherwise same plasma parameters, have been simulated for the fan of rays allowed by the selected geometry. It is noted here that intersection of the line-of-sights with the magnetic surfaces in the plasma is approximated as a two-dimensional problem, that is the toroidal coordinate is ignored as a first approximation. The plasma electron temperature and density profiles are given by parametric expressions:

$$T_e = (T_0 - T_a)(1 - x^2)^{\gamma_T} + T_a$$

$$n_e = (n_0 - n_a)(1 - x^2)^{\gamma_n} + n_a$$

where the subscript 0 refers to the central value, and the subscript *a* to the value at the last closed magnetic surface (LCMS). The magnetic surfaces themselves are described by the equations:

$$\begin{cases} R_{i,\theta} = a_i \cos(\theta + \delta_i \sin(\theta)) + R_{i,0} \\ z_{i,\theta} = (\kappa_i a_i) \sin(\theta) + sh \end{cases}$$

where the parameters R_0, a, δ, κ are interpolations of actual equilibrium calculations, and θ is the poloidal angle. The parameter *sh* represents the downward (or upward) shift of the magnetic surfaces that will be used to simulate the loss of vertical control. In the reference position, the only contact point of the LCMS with the First Wall is on the inner midplane. When the plasma is shifted downwards, that point is taken to be the lowest one in the vessel, while the parameters *R* and *a* are adjusted slightly for the LCMS not to touch the wall anywhere else. Initially, the temperature and density profiles have been left the same. This is to verify that the minimal change of position could be distinguished from other plasma effects. However, the combined effects of loss of vertical control and increased/decreased temperature and/or impurity density have yet to be explored. Another important simplification was to neglect the emission from the plasma volume in the SOL (Scrape-Off Layer) that in Ignitor plays a very significant role in reducing the thermal wall loads.

The emission along the line of sights is calculated assuming a constant density of Mo ions

$$P_{Mo} = n_e n_{Mo} L_{cr}(T_e) \times 10^{21} \text{ (MW/m}^3\text{)},$$

with n_{Mo} = 6×10^{-4} (in units of 10^{20} m^{-3}) and the total radiative cooling rates $L_{cr}(T_e)$ from Ref. [vi]. The power radiated by bremsstrahlung, for a constant Z_{eff} = 1.2, is calculated separately from the total emission of Mo,

$$P_{brem} = 1.7\times10^{2}\left(Z_{eff} n_e\right)^2 T_{e,eV}^{1/2} \ (\mathrm{MW/m^3}),$$

and it is found to give a negligible contribution for these peripheral chords. Finally, the emission for a particular line, the electric dipole E1 transition $3d^{9}{}_{5/2}4p_{3/2} \rightarrow 3d^{10}$ of Mo^{14+} at 50.444 Å [x] is considered,

$$P_{Mo14E1} = 1.6\times10^{-4} n_e n_{Mo} f_{Mo14} Q_{E1} \Delta E_{E1} \ (\mathrm{MW/m^3}),$$

where f_{Mo14} is the fractional abundance of Mo^{14+}, $Q_{E1}(T_e)$ is the transition excitation rate, and ΔE_{E1} is the transition energy.

In Fig. 5a the profile of the total emission integral *at the crystal* is shown as function of the line-of-sight angle, for three different locations of the crystal, for the plasma column in the reference position (open symbols) and the plasma shifted to the bottom (solid lines). It is clear that for the more central line-of sights the small change in the magnetic surface geometry produces an insignificant variation in the signal, whereas the more "vertical" observation is much more sensitive. The reason can essentially be attributed to the step in the Mo cooling rate at 50 eV (Fig. 2). Since the LCMS in Ignitor is expected to be right around this value, the maximum sensitivity to a shift of the magnetic configuration is observed when the line-of-sights fan across the 50 eV region.

A similar variation of signal intensity is calculated for the dipole line E1, whose brightness profile presents a different shape, with a strong peak at the very edge of the range of observation (Fig. 5b). From these plots, it is obvious that when the crystal is closer to the plasma, taking a more vertical view of it, then it is also more sensitive to its movements. On the other hand, the closer it is, the more exposed to the radiation and particle fluxes the crystal become, with an increase risk of damage. For now, we have selected the position of **C** at [2.050,0,0], as this seems to provide an adequate contrast while still being comfortably tucked away inside the port.

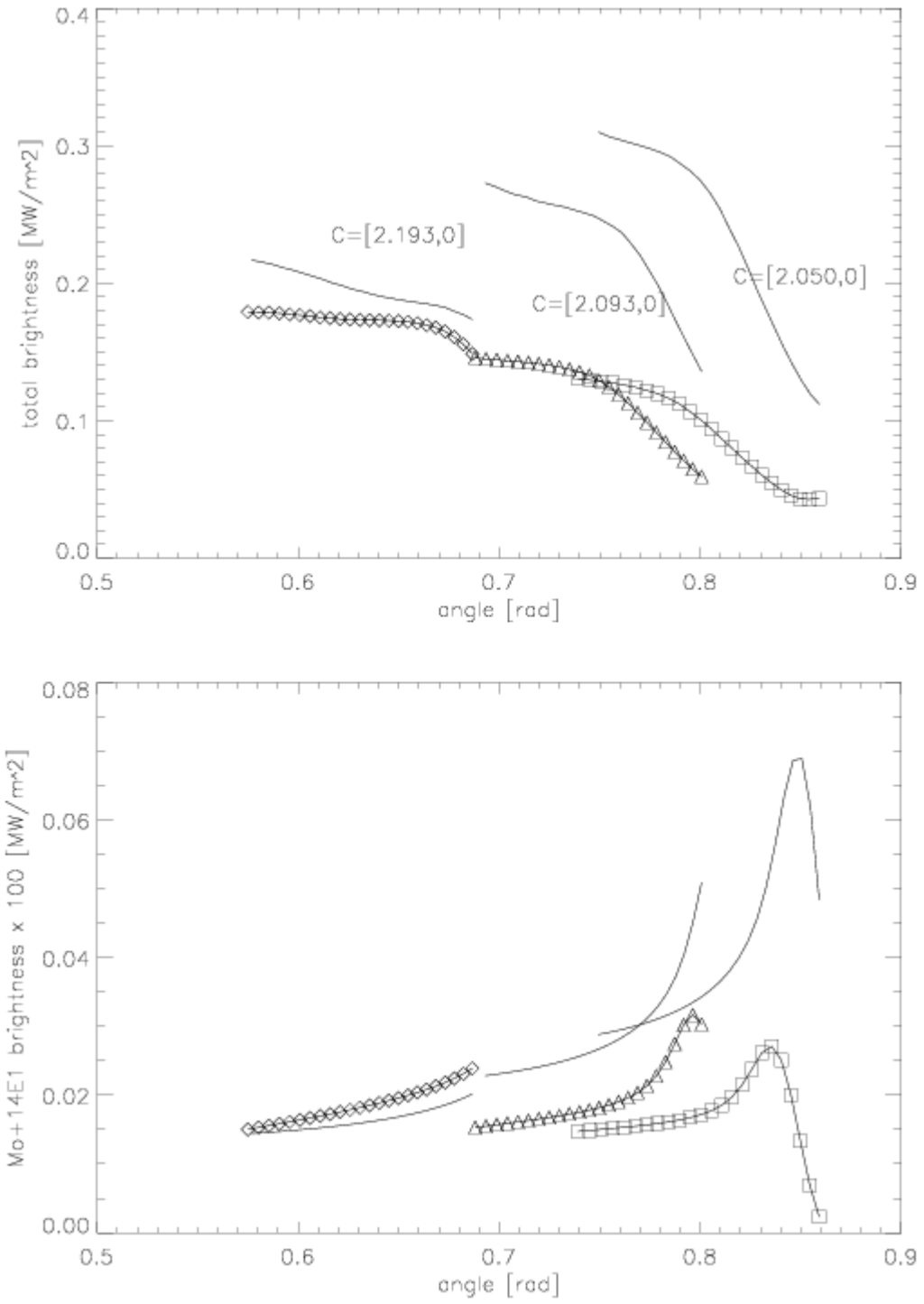

Fig. 5 Line integrated signal for three different positions of the diffracting element. (a, top): total signal, (b, bottom): line $3d^{9}_{5/2}4p_{3/2} \rightarrow 3d^{10}$ *of* Mo^{14+} *at 50.444 Å. The symbols show the profile when the plasma is in the reference position, the solid lines*

V. Instrument Throughput

In order to verify the adequacy of the chosen lay-out, it is important to estimate the system throughput, since that determines the time resolution of the measurement. A procedure similar to that adopted in Ref. [xi] is followed.

The counting rate at the detector is a function, other than of the source emissivity, of the system geometry, of the MLM reflectivity, of the slit aperture, and of the detector efficiency. Furthermore, absorption along the optical path by Be windows and air gaps have to be accounted for. The counting rate ν (Hz) is given by:

= olution solid state detectors have been developed by PSI [xii], with very interesting characteristics, but we are looking at the more versatile GEM (Gas Electron Multiplier) detector developed at CERN [xiii]. Its application for plasma imaging in fusion experiments has been already successfully tested [xiv] on fusion experiments.

The basic principle of operation of a GEM detector is illustrated in Fig. 8. The GEM foil can be made in any size, but for practical purposes we think that a 10 x 10 cm^2 is adequate for our application. The intrinsic resolution is very high, but it is the rear read-out pads that determined the effective spatial resolution and the type of electronics to be installed.

The detector can be run either in single photon count mode, or in current mode, if the photon flux is sufficiently high. Contrary to the high resolution set-up, for this application the read-out pads will have a higher resolution in the "vertical" direction than in the spectral plane. The simulations carried out so far have assumed 24 vertical channels and a signal integrated over the whole horizontal width of the detector. In practice it may be useful to have few horizontal channels (of the order of 8) to distinguish at least roughly the main spectral features of the collected signal, for proper alignment. This arrangement should allow a spatial resolution of about 5 mm and a field of view of about 15 cm in the poloidal plane.

VI. Multilayer Mirrors

Multilayer Mirrors (MLM) are made of two different materials, a diffracting one, of atomic number ZA and the other non-diffracting, of atomic number ZB, alternating in layers of

(usually different) thickness dA and dB. The period of the Multilayer is given by the total thickness of the layers, dA + dB, in the direction perpendicular to the diffracting planes. In other words, the non-diffracting plane acts as a spacer, and interatomic distances between 20 and 200 Å. The shortest wavelength that a MLM can diffract is limited by the minimum thickness of the diffracting layer that can be manufactured, while the longest wavelength that can be resolved depends on the absorption coefficients of the adopted materials.

The main advantage of the MLM over natural crystals is obviously the reflectivity, which can be improved by adjusting the relative thickness of the two materials. Also the effects of absorption can be minimized by an appropriate choice of the elements forming the multilayer. The major drawback is the poor resolving power, which should not be a real hindrance for the present application. By making use of numerical tools available on the web [xv], we have estimated an integrated reflectivity of about 10% for a MLM made of Ni/C with a period of 9.4 nm and ratio 0.6.

VII. Control System

The plasma position and shape of the plasma column is controlled by the external poloidal field coils. The capability of the system, as presently designed, to provide an effective vertical stabilization has been investigated using the CREATE_L linearized response model [xvi]. This model assumes that the system is axisymmetric and that the interaction of the plasma with the surrounding structures is described by a small number of global parameters (β_{pol}, internal inductance l_i, and plasma current I_p). Using this model, a PID vertical position controller has been designed to stabilize the system against sudden vertical displacements of the order of 5 mm both with a voltage and a current loop control scheme. All the main features of the power supplies have been taken into account, including the time delays (around 1 ms) that are one of the major bottlenecks in achieving better control performances [ii]. A linear combination of signals from a set of 20 poloidal field sensors and 20 for the flux is used to determine the vertical position of the plasma column. The diagnostic system described in this paper will have to provide an equivalent set of signals to supplement or replace the magnetic data in case of failure due to high radiation background.

Our first step was to assume a rigid vertical shift of the plasma column to simulate the change in plasma emissivity along a fan of chords. *Per se* this information may not be sufficient to establish the shape of the plasma column, whereas the dramatic variation of the signal shown in Figs 5 could be used, with an appropriate algorithm, as input to the feedback system for monitoring the plasma vertical position. By tracking the level of emission with its spatial and temporal distribution a fairly precise assessment of the plasma movements should be possible. The relevant simulations aimed at establishing the sensitivity of the measurement also to changes in other plasma parameters will be the subject of a following paper.

Acknowledgments

This work is supported in part by ENEA and Università di Bary of Italy and by the US DOE. Special thanks to Dr. P. Gorenstein, of the Harvard-Smithsonian Center for Astrophysics for his advice regarding Multi Layer Mirrors, and to Prof. B. Coppi and Prof. Capitelli for their unreserved support.

References

[i] B. Coppi, A. Airoldi, F. Bombarda, et al., *Nucl. Fusion* **41(9)**, 1253 (2001).
[ii] G. Ramogida, R. Albanese, F. Alladio, et al., *Proceed. of 24th SOFT Conference,* Warsaw (Poland), 2006, Paper P2-C-233.
[iii] C. Ferro, etc
[iv] S. Pitcher
[v] Post, Jensen, Atomic Data and Nuclear Data Tables
[vi] Fournier, Pacella, *Nucl. Fusion*
[vii] R. Bartiromo, F. Bombarda, M. Leigheb, et al., in "Diagnostics for Contemporary Fusion Experiments", P.E. Stott, D.K. Akulina, G. Gorini and E. Sindoni, (Eds.), p. 959, SIF, Bologna (1991).
[viii] M. Bitter, B. Fraenkel, K.W. Hill, et al., *Rev. Sci. Instrum.* **66**, 530 (1995).
[ix] D. Pacella, R. Bellazzini, A. Brez, et al., *Nucl. Instrum. & Methods A* **508,** 414 (2003)
[x] M. Klapisch, J.L. Schwob, M. Finkental, et al., *Phys. Rev. Letters* **41,** 403 (1978)
[xi] R. Bartiromo, et al., CNEN Report 80.31, Associazione Euratom-CNEN sulla Fusione, Frascati, Italy (1980)
[xii]Ch. Broennimann, E. F. Eikenberry, B. Henrich, *J. Sinchrotron Rad.* **13**, 120 (2006)
[xiii] F. Sauli, *Nucl. Instrum. Meth. A* **419**, 189 (1998)
[xiv] D. Pacella, R. Bellazzini, A. Brez, et al., *Nucl. Instrum. Meth A*, **508**, 414 (2003)
[xv] http://www-cxr0.lbl.gov/optical_constants/multi2.html
[xvi] R. Albanese, F. Villone, *Nucl. Fusion* **38(5)** 723 (1998)